Japanese Journal of Radiology (2019) 37:701–709
https://doi.org/10.1007/s11604-019-00861-z

ORIGINAL ARTICLE

Assessment of angiogenesis in rabbit orthotropic liver tumors using three-dimensional dynamic contrast-enhanced ultrasound compared with two-dimensional DCE-US

Qiao Zheng[1] · Jian-chao Zhang[1] · Zhu Wang[1] · Si-Min Ruan[1] · Wei Li[1] · Fu-Shun Pan[1] · Li-Da Chen[1] · Yu-Chen Zhang[2] · Wen-Xin Wu[2] · Xiao-Yan Xie[1] · Ming-De Lu[1,3] · Quan-Yuan Shan[1] · Wei Wang[1]

Received: 18 January 2019 / Accepted: 26 July 2019 / Published online: 10 August 2019

Abstract

Objectives To evaluate quantitative three-dimensional (3D) dynamic contrast-enhanced ultrasound (DCE-US) in the assessment of tumor angiogenesis using an orthotropic liver tumor model.

Methods Nine New Zealand white rabbits with liver orthotropic VX2 tumors were established and imaged by two-dimensional (2D) and 3D DCE-US after SonoVue® bolus injections. The intraclass correlation coefficients of perfusion parameters, including peak intensity (PI), mean transit time, time to peak, and area under the curve, were calculated based on time-intensity curve. The percentage area of microvascular (PAMV) and the expression of vascular endothelial growth factor (VEGF) were both evaluated by immunohistochemical analysis and weighted by the tumor activity area ratio. Correlations between quantitative and histologic parameters were analyzed.

Results The reproducibility of 3D DCE-US quantitative parameters was excellent (ICC 0.91–0.99); but only PI showed high reproducibility (ICC 0.97) in 2D. None of the parameters of quantitative 2D DCE-US were significantly correlated with weighted PAMV or VEGF. For 3D DCE-US, there was a positive correlation between PI and weighted PAMV ($r = 0.74$, $P = 0.04$) as well as VEGF ($r = 0.79$, $P = 0.02$).

Conclusion Quantitative parameters of 3D DCE-US show feasibility, higher reproducibility and accuracy for the assessment of tumor angiogenesis using an orthotropic liver tumor model compared with 2D DCE-US.

Keywords Ultrasonography · Three-dimensional imaging · Pathologic neovascularization · Assessment

Abbreviations

au	Arbitrary units
AUC	Area under the curve
DCE-US	Dynamic contrast-enhanced ultrasound
ICC	Intraclass correlation coefficient
MTT	Mean transit time
PAMV	Percentage area of microvascular
PI	Peak intensity
ROI	Region of interest
3D	Three-dimensional
TIC	Time-intensity curve
TTP	Time to peak
2D	Two-dimensional
VEGF	Vascular endothelial growth factor
VOI	Volume of interest

Qiao Zheng and Jian-chao Zhang contributed equally to this study.

Electronic supplementary material The online version of this article (https://doi.org/10.1007/s11604-019-00861-z) contains supplementary material, which is available to authorized users.

✉ Quan-Yuan Shan
shanqy3@mail.sysu.edu.cn

✉ Wei Wang
wangw73@mail.sysu.edu.cn

Extended author information available on the last page of the article

Introduction

Angiogenesis, which is important in tumor progression, is one of the main elements in carcinoma early diagnosis, precise staging, treatment options selection and patient monitoring [1]. Anti-angiogenic therapies have been developed and demonstrated as valuable methods against tumor neovascularization. Currently, the treatment assessment of non-surgical therapies in cancer patients is

still based on the Response Evaluation Criteria in Solid Tumors (RECIST), which relies on tumor size changes [2]. However, as for anti-angiogenic therapies, anatomical changes of tumors may not occur in months. To minimize patient costs and maximize tumor responses by therapeutic regimen adjustment, functional and molecular imaging approaches are needed in evaluating early changes in tumor blood perfusion.

Diagnostic modalities, such as dynamic contrast-enhanced computed tomography (DCE-CT), positron emission tomography with computed tomography (PET-CT), dynamic contrast-enhanced magnetic resonance imaging (DCE-MRI) and dynamic contrast-enhanced ultrasound (DCE-US), have shown usefulness in tumor angiogenesis assessment separately and in combination [3]. Among these techniques, DCE-US has several advantages, such as relatively low cost, non-invasiveness, excellent spatial and temporal resolution, and non-ionizing irradiation. DCE-US is more likely to be used as a routine tool for tumor imaging. Moreover, gas-encapsulated microbubbles, as blood pool contrast agents, show potential in perfusion quantification [4]. Quantitative DCE-US can improve diagnostic efficacy by analyzing time-intensity curves following bolus injections of microbubbles [5], which avoids the drawbacks of DCE-US, including over-reliance on the experience and subjectivity of the examiners. In literature review, quantitative analyses of DCE-US were mainly based on two-dimensional (2D) imaging [6, 7] and had been used in both pre-clinical and clinical studies. By evaluating the post-treatment changes of quantitative parameters, early treatment responses could be visualized in models of breast cancer [8], colon cancer [9] and hepatoma [10] before tumor sizes were affected. Nevertheless, influenced by necrosis, hypoxia and other circumstances, which might cause heterogeneous tumor perfusion, the stability and veracity of quantitative 2D DCE-US were doubted [11], and three-dimensional (3D) data sets were required in quantitative analysis [12].

Recent studies had shown that quantitative 3D DCE-US could be used in early anti-angiogenic treatment assessment in subcutaneous colon cancer xenografts in mice [13] and could help distinguish responders from non-responders as early as 24 h after treatment initiation [14]. However, subcutaneous colon cancer models did not represent the tumor microenvironment, and orthotopic liver tumor models were needed. In addition, the reproducibility of 3D DCE-US quantitative parameters was also tested in patients with liver metastases and was highly repeatable and feasible [15], without confirming the accuracy based on histological findings.

The objective of the present study was to verify the feasibility, accuracy and stability of quantitative 3D DCE-US in tumor angiogenesis assessment using rabbit VX2 liver tumor models and optimize the pathological evaluation of tumor angiogenesis.

Materials and methods

Animal models

Approved by the Animal Research Ethics Committee of our university, the experiments were conducted with nine New Zealand white rabbits weighting 2.0–2.5 kg. Consistent with previous studies, nine rabbits were anesthetized by 3% pentobarbital sodium (1 ml/kg) through auricular vein injection. After median abdominal incision and liver exposing, VX2 tumor tissue cubes (diameter 2 mm) were implanted into the liver (left lobe) of each rabbit to establish a VX2 model. All rabbits were individually weighed before imaging.

Imaging protocol

After implantation, tumor progression was monitored using an ultrasound machine (Aplio 500, Canon Medical Systems, Tochigi, Japan) with a linear probe (PVT-805AT, frequency 7.5 MHz, Canon Medical Systems, Tochigi, Japan). When the diameter of the tumor reached 1 cm, the rabbits were subjected to the following US procedure.

Rabbits under intravenous anesthesia through auricular vein injection (3% pentobarbital sodium, 1 ml/kg) were placed supine on a heated stage during scanning to maintain constant body temperature. Conventional US was performed using Aplio 500 and a 3D imaging probe (PVT-375MV) to record the basic characteristics of the tumors (including number, size, boundary, shape and echogenicity, etc.). Subsequently, DCE-US was performed from the maximum plane of each lesion. As it is difficult to demarcate the tumor with normal liver parenchyma correctly in the normal ultrasound images, we determined the border in contrast-enhanced US image. All of the parameters of both 2D and 3D DCE-US were set as shown in Table 1. A bolus injection of SonoVue® (1 ml/kg) was administered via the auricular vein through a 21-G peripheral intravenous catheter, followed by a 5-ml saline flush. Both 2D and 3D DCE-US were respectively repeated twice, and 3 min of raw data clips were continually stored right after the bolus injection of UCA. A 30-minute break was observed between each injection in addition to a high mechanical index insonation.

Imaging analysis

Online analysis software package accompanied by ultrasound (Aplio 500, Version 3.7, CHI-Q, Canon Medical Systems, Tochigi, Japan) was used for imaging analysis. In 2D DCE-US, a region of interest (ROI) was drawn to obtain the associated time intensity curve (TIC). For each image,

Table 1 Imaging parameters of 2D and 3D DCE-US

Parameter	2D DCE-US	3D DCE-US
Imaging technique	CHI	CHI
Mechanic index	0.09	0.09
Frequency (MHz)	3.5	3.5
Gray density (dB)	78	78
Dynamic range	60	60
Frame rate	10 frame/s	1.5 volume/s
Focal point	1	1
Focus location	Tumor	Tumor
Acoustic power output (%)	2	2

2D two-dimensional, *3D* three-dimensional, *DCE-US* dynamic contrast-enhanced ultrasound, *CHI* contrast harmonic imaging, *MHz* megahertz, *dB* decibel

target ROI (tROI) (draw along the margin of the lesion) and reference ROI (rROI) (including surrounding liver parenchyma with the same volume and depth as tROI, avoiding large blood vessels) were respectively drawn. In 3D DCE-US, a volume of interest (VOI) was delineated by covering the entire lesion visualized on sagittal, axial, and coronal planes. Target VOI (tVOI) and reference VOI (rVOI) were also manually contoured. TICs were obtained from analysis software by two skillful investigators (W.W. and L.D.C, each of whom has more than 10 years of experience in liver CEUS) and quantitative parameters, including peak intensity (PI), mean transit time (MTT), time to peak (TTP) and area under the curve (AUC), were automatically calculated. PI was defined as the highest signal intensity of contrast agent after bolus injection in ROI/VOI. MTT was defined as the mean time from perfusion to the clearance of contrast agent. TTP was defined as the time interval from occurrence to maximum signal intensity. AUC was defined as the area under the curve of TIC, which represents the total perfusion volume of ROI/VOI.

Histology analysis

The rabbits were euthanized with an overdose of 3% pentobarbital sodium and subsequently dissected after DCE-US examinations. Tumors as well as surrounding liver parenchyma were excised and fixed in formalin solution. Paraffin-embedded sections were prepared and stained with hematoxylin–eosin (HE). Immunohistochemical staining with a CD34 rabbit polyclonal antibody (ratio 1:400; Hopebiot, JiangSu, China) was used to label vascular endothelial cells. Vascular endothelial growth factor (VEGF) immunohistochemical staining was performed using a monoclonal antibody against VEGF (ratio 1:400; Novusbio, USA). Pathological images were saved and observed by pathologists with 10 years of experience.

In consideration of the feasibility and importance in assessing tumor activity, the percentage area of microvascular (PAMV) and VEGF expression scores were selected as reference pathological parameters to evaluate angiogenesis level.

PAMV was assessed in the following manner [16]. CD34 immunohistochemical staining was performed under a microscope (200×-power), and five visual fields in the non-necrotic area of the tumor were randomly selected. Image analysis software (ImageJ, 1.42q, National Institutes of Health, USA) was used to calculate the area ratio of microvascular to each visual field, or PAMV (%) of the field. Next, the mean value of five field PAMVs was multiplied by the tumor active area ratio to obtain the weighted PAMV (%) of the specimen. The tumor-active ratio was performed using the following equation:

$$\text{Tumor activity area ratio} = \frac{\text{Area}_{\text{entire tumor}} \quad \text{Area}_{\text{necrosis}}}{\text{Area}_{\text{entire tumor}}}.$$

VEGF expression scores were calculated in the following manner [17]. According to the semi-quantitative method, the ratio of positively stained cells (1 point for < 25%, 2 points for 26–50%, 3 points for 51–75% and 4 points for > 75%) as well as the staining intensity (0 point for no staining, 1 point for light yellow, 2 points for yellow and 3 points for brown) was respectively scored. The final score was calculated as the sum of the above two scores: 0–1 point as negative (−), 2–3 points as weakly positive (+), 4–5 points as medium positive (++) and 6–7 points as strongly positive (+++). Among these scores (−) and (+) were recorded as the low expression group, and (++) together with (+++) were recorded as the high expression group. The resulting score was then multiplied by the tumor-active area ratio to obtain the weighted VEGF score.

Statistical analysis

Continuous data were expressed as the mean values ± SD. Intraclass correlation coefficient (ICC) (0–0.20, no agreement; 0.21–0.40, poor agreement; 0.41–0.61, moderate agreement; 0.51–0.80, good agreement; and > 0.80, excellent agreement) and 95% confidence intervals were calculated to assess the reproducibility of quantitative 2D and 3D DCE-US between the two injections. Spearman's correlation coefficient (r) between tumor perfusion parameters and angiogenesis level (weighted PAMV as well as VEGF scores) were obtained to evaluate the accuracy. The significance level was set at 0.05. Statistical analyses were performed by SPSS 19.0 software (SPSS Inc., Chicago, IL, USA).

Results

Animal model establishment

An imaging protocol was performed in every three rabbits at three time points, namely, 2, 3 and 4 weeks after implantation, to ensure that different-sized tumors were obtained. Overall, nine tumors with various sizes were observed (diameter 1.5 ± 0.5 cm, range 1.1–2.4 cm), all of which were located in the left lobe of the liver, and these tumors exhibited heterogeneous hypo echogenicity in conventional US and with little blood flow signal in color Doppler flow imaging. In DCE-US, the tumors showed heterogeneous hyper-enhancement in 7–11 s after the bolus injection of UCA and rapid wash-out in 15–25 s (Figs. 1, 2).

Angiogenesis evaluation

Rabbit VX2 liver tumors were round or oval nodules with yellowish liquefaction necrosis surrounded by fish-like tissues. In sections, nest-like to beam-like tumor cells were observed with clear boundaries to normal tissues, and necrotic areas of various sizes were observed in the center (Fig. 3). One of the nine tumors did not show active tumor cells other than necrosis, and thus, this tumor was not included in subsequent analyses.

Microvascular endothelial cells were stained brown under immunohistochemical staining with CD34, densely

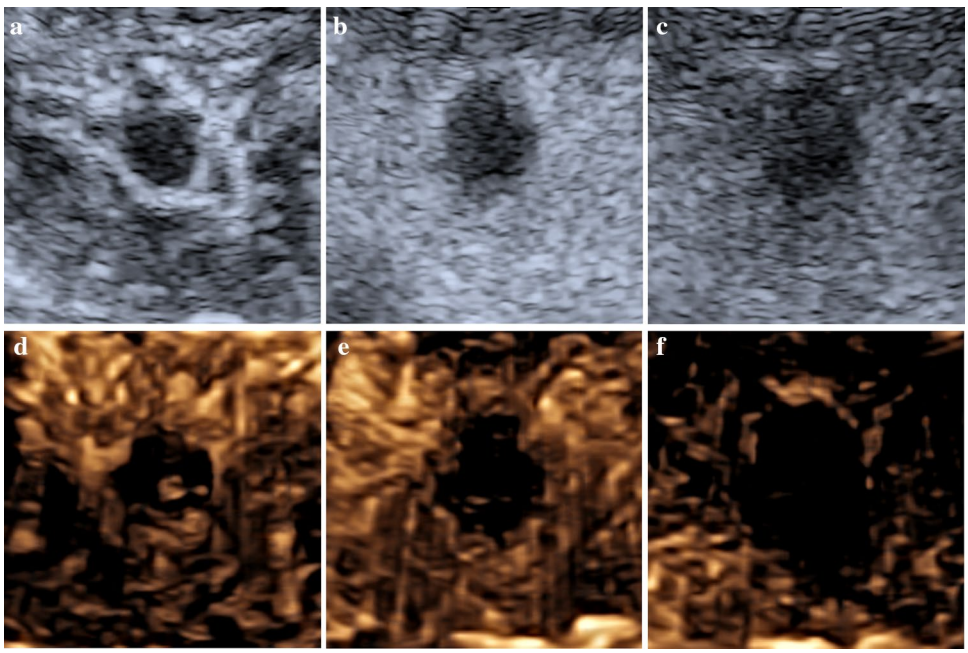

Fig. 1 2D and 3D dynamic contrast-enhanced ultrasound (DCE-US) images of a rabbit VX2 liver tumor in arterial (7 s) (**a**, **d**), portal (24 s) (**b**, **e**) and late phase (60 s) (**c**, **f**). Tumor showed rim-like heterogeneous hyper-enhancement in the arterial phase and wash-out as hypo-enhancement in the portal phase. The center portion of necrosis showed no enhancement during three phases

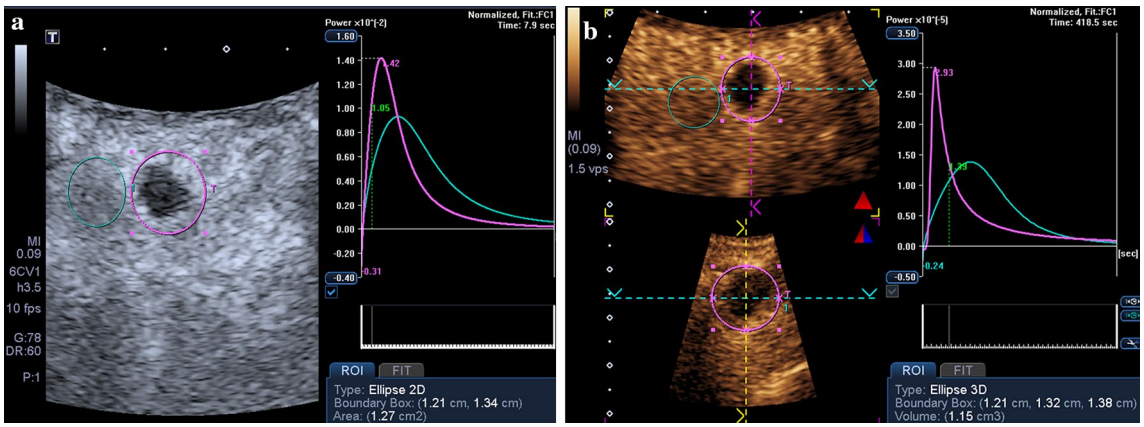

Fig. 2 Time-intensity curves (TIC) of 2D (**a**) and 3D (**b**) dynamic contrast-enhanced ultrasound of a rabbit VX2 liver tumor. The pink parabola—TIC of the tumor. The blue parabola—TIC of liver parenchyma. Both TICs showed similar enhancement pattern

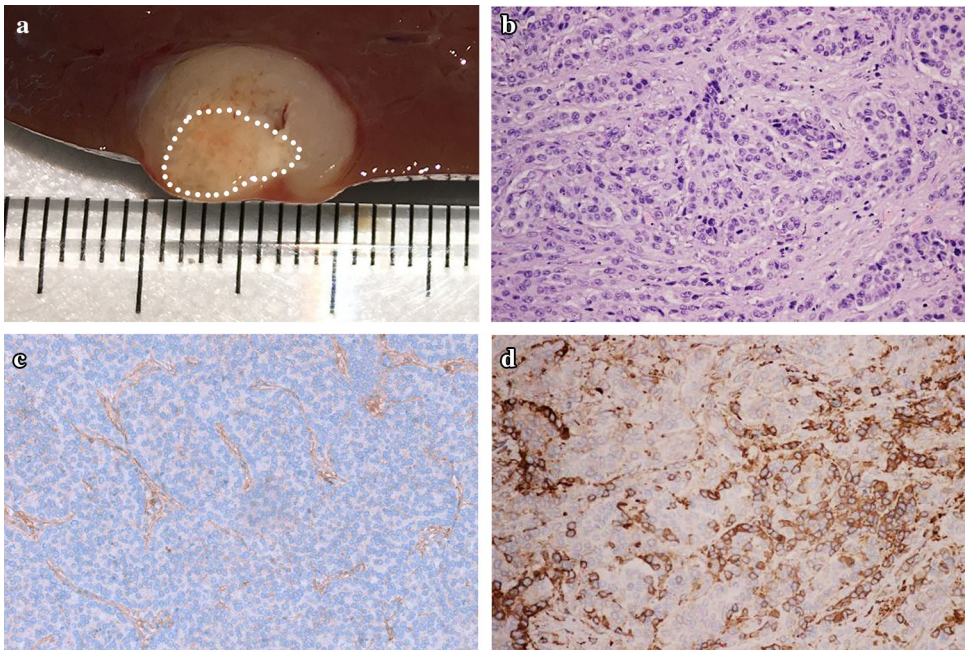

Fig. 3 **a** Macroscopic appearance of a rabbit VX2 liver tumor (diameter 1.2 cm) with significant necrosis (area with white dotted boundary). **b–d** Representative photomicrographs of tumor sections: **b** hematoxylin–eosin staining; **c** immunohistochemical staining of CD34 rabbit polyclonal antibody (endothelial cells were brown stained); **d** immunohistochemical staining of vascular endothelial growth factor monoclonal antibody. (Original magnification, ×400-power.)

distributed in the peripheral area of the tumor, adjacent to the normal liver parenchyma (Fig. 3). ImageJ software was used to analyze these sections and obtain the original and weighted PAMV of each sample (Fig. 4). In addition, all tumors were VEGF-positive with different staining intensities and proportions of positive cells (Fig. 3). Three specimens were pale yellow and the remaining specimens were brown; the proportion of positive cells was < 25% in one specimen, 51–75% and > 75% in each two specimens, and 26–50% in three specimens. In total, three specimens were categorized into the low-expression group, and five specimens were categorized into the high-expression group.

Reproducibility comparison between quantitative 2D and 3D DCE-US

The mean actual raw data of quantitative parameters including PI, TTP, MTT, AUC in twice examinations on 2D and 3D US in respective tumors were presented in the supplementary Table 1 and supplementary Table 2. The reproducibility of 3D DCE-US quantitative parameters (PI, TTP, MTT, and AUC were included) was excellent (ICC 0.91–0.99). The differences among the 3D perfusion parameters measured from two bolus injections were not significant. However, in quantitative 2D DCE-US, only PI showed good agreement (ICC 0.97), while TTP, MTT, and AUC did not show good agreement through experiments (Table 2).

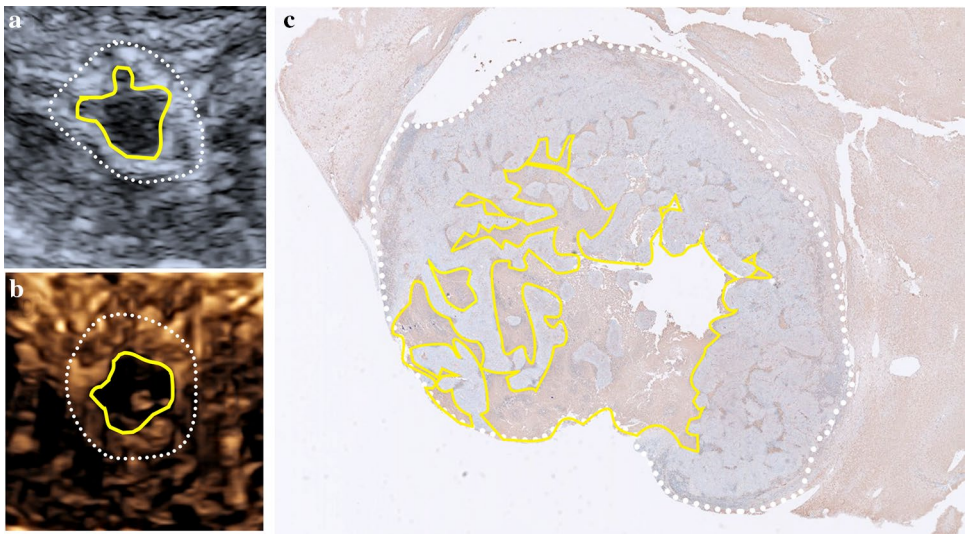

Fig. 4 Comparison of 2D (**a**) and 3D (**b**) dynamic contrast-enhanced ultrasound images in arterial phase and histologic image (**c**) (stained with CD34) of a rabbit VX2 liver tumor (area within white dotted boundary). Significant irregular necrosis were visible (area within yellow boundary)

Table 2 Quantitative parameters obtained using 2D and 3D DCE-US in rabbit VX2 liver tumors each scanned twice

Quantitative parameter	ICC	*P* value*
2D DCE-US		
PI (au)	0.97 (0.86,0.99)*	0.19
TTP (s)	0.56 (−1.19,0.91)*	0.57
MTT (s)	0.79 (−0.05,0.96)*	0.86
AUC (au)	0.29 (−2.54,0.86)*	0.26
3D DCE-US		
PI (au)	0.99 (0.93,0.99)*	0.52
TTP (s)	0.91 (0.55,0.98)*	0.23
MTT (s)	0.96 (0.78,0.99)*	0.45
AUC (au)	0.94 (0.69,0.99)*	0.68

2D two-dimensional, *3D* three-dimensional, *DCE-US* dynamic contrast-enhanced ultrasound, *ICC* Intraclass correlation coefficient, *PI* peak intensity, *TTP* time to peak, *MTT* mean transit time, *AUC* area under the curve, *au* arbitrary units, *s* seconds

*P values refer to differences between two scans. Data in parentheses are 95% confidence intervals

Accuracy comparison between quantitative 2D and 3D DCE-US

According to Spearman's correlation test, none of the parameters of quantitative 2D DCE-US, including PI, TTP, MTT, and AUC, were significantly correlated with weighted PAMV or VEGF ($P > 0.05$). Additionally, as for 3D DCE-US, there was a positive correlation between PI and weighted PAMV ($r = 0.74$, $P = 0.04$) as well as VEGF ($r = 0.79$, $P = 0.02$) (Table 2). TTP, MTT, and AUC were not correlated with the pathological results in quantitative 3D DCE-US ($P > 0.05$).

Discussion

In the present study, the quantitative 3D DCE-US parameters, including PI, TTP, MTT, and AUC, were highly repeatable. Among these parameters, PI showed a positive correlation with histological weighted PAMV and VEGF. The present study also demonstrated an improved method to weigh histological tumor neovascularization parameters with activity area ratios.

Quantitative DCE-US can objectively analyze both wash-in and wash-out of UCA through TIC, which has been confirmed as useful in the treatment response assessment of cancer patients. This method could be used to detect tumor perfusion changes in metastatic renal carcinoma patients undergoing Sunitinib treatment for 15 days [18] and in hepatocellular carcinoma patients receiving Bevacizumab for only 3 days [19]. However, the results of quantitative 2D DCE-US could show a lack of stability for being highly correlated with the selected imaging planes, which had variable perfusion levels and were prone to sampling errors. Studies have shown that quantitative results variance in cross-section could be as high as 22% in the kidneys of healthy mice [20]. Moreover, the uneven distribution of tumor blood vessels could also result in quantitative errors [21]. Wang et al. found that quantitative analysis based on central 2D DCE-US imaging could either over- or underestimate treatment responses in mouse colon cancer compared with the volumetric data set [16]. Additionally, the requirement for maintaining the imaging plane during long-term follow-up is also the lack of clinical operability.

In contrast, 3D DCE-US can assess tumor perfusion based on the whole lesion and thus minimize sampling errors [16]. The feasibility and reproducibility of 3D DCE-US quantitative parameters were promising in patients with liver metastases [15]. In subcutaneous colon cancer xenografts in mice, changes in PI, VEGFR2 expression and the percentage area of blood vessel were obvious between quantitative 3D DCE-US obtained at baseline and at 24 h after Bevacizumab treatment [13]. Zhou et al. found that the PI and AUC of 3D DCE-US were sensitive in assessing early treatment response, and could help to distinguish classifying responders from non-responders as early as 24 h after treatment initiation [14]. However, the authors concluded that the subcutaneous colon cancer model could not represent the tumor microenvironment, and orthotopic liver tumor models were needed (Table 3).

In the present study, we compared the stability and accuracy between quantitative 2D and 3D DCE-US through in vivo experiments using a rabbit VX2 liver tumor model. The left hepatic lobe of rabbit is the largest lobe, which is easy to be operated, and easy to image. And the median abdominal incision is facing the left hepatic lobe. In addition to the left lobe, there are also some literatures that plant tumors in the middle lobe, but our research group used to select the left lobe when establishing the VX2 tumor model [22]. The operation is convenient, the model is stable, and the effect is good. Therefore, the left lobe is still selected in this experiment. Few US contrast agents are available on the market for performing CEUS studies. SonoVue is ultrasound contrast that has been widely used in Europe and parts of Asia for almost 15 years [23]. SonoVue is made up of microbubbles (2–10 μm) with a shell of phospholipids that are filled with sulfur hexafluoride gas, which is confined in the vessels after the injection, presents a high reflectivity with a low mechanical index and allows the visualization of the tiny vessels in the capillary bed, thus permitting the dynamic detection of capillary microvascularization. That is why we selected SonoVue as contrast agent. Mice tumors are too small for ultrasound examination, so the rabbit was chosen as experimental animal and our research group had established a stable VX2 model in the rabbit [22].

Table 3 Correlation between quantitative parameters of 2D and 3D DCE-US and histologic results in rabbit VX2 liver tumors

DCE-US	Parameter[a]	PI		TTP		MTT		AUC	
		R value	*P* value	*R* value	*P* value	*R* value	*P* value	*R* value	*P* value
2D	PAMV	0.55	0.16	−0.12	0.78	−0.62	0.1	0.43	0.29
	VEGF	0.64	0.09	0.14	0.74	−0.24	0.57	0.48	0.23
3D	PAMV	0.74	0.04	0.41	0.32	0.38	0.35	0.19	0.65
	VEGF	0.79	0.02	0.62	0.1	0.38	0.35	0.41	0.32

2D two-dimensional, *3D* three-dimensional, *DCE-US* dynamic contrast-enhanced ultrasound, *PI* peak intensity, *TTP* time to peak, *MTT* mean transit time, *AUC* area under the curve, *PAMV* percentage area of microvascular, *VEGF* vascular endothelial growth factor

[a]PAMV and VEGF were all weighted by tumor activity area ratio in each case

For stability, we respectively analyzed the quantitative parameters in two scans. The results showed that quantitative parameters of 3D DCE-US were well consistent in multiple measurements and showed a significantly superior repeatability to 2D, suggesting that 3D DCE-US could bring an effective reduction of error caused by section variation.

As an important means of tumor diagnosis and prognosis prediction, the qualitative as well as quantitative detection of tumor neovascularization has been studied in recent decades. Weidner et al. established a method for evaluating microvascular density (MVD) [24], according to which a number of studies have shown that the prognoses of patients with breast cancer and non-small cell lung cancer were significantly correlated with tumor MVD [25–27]. Subsequently, the MVD counting method was gradually diversified, but all methods were still based on "hot spots", or areas with the largest number of microvessels under optical microscopy, and the mean value was taken as the MVD value (/mm^2) of the specimen. Therefore, MVD could only represent the "highest level" of tumor angiogenesis, and the selection of "hot spots" both pathologically and in DCE-US images is subjective, and both of which will bring bias to accuracy evaluation. In addition, according to a study by Shree S., PAMV was a better prognostic marker for renal cell carcinoma than MVD, as PAMV significantly increased with increasing stage of tumors, while MVD did not [28]. This result might arise from an increase in the blood vessel diameter rather than the density in higher-stage tumors [28]. Thus, in the present study, we used PAMV as one of the tumor neovascularization parameters. The observed areas of PAMV were randomly selected instead of limited to "hot spots".

In previous studies on quantitative DCE-US, the selection of target ROI was based on the following principles: for non-necrotic tumors, ROI should contain the entire tumor [29]; for internally necrotic tumors, ROI should be placed in the non-necrotic area with the highest level of enhancement in the arterial phase [30]). In the present study, we selected the entire tumor rather than the highest enhanced region as the target ROI, and the necrosis area of which would bring a reduction to quantitative parameters, such as PI, AUC, etc. However, not affected by necrosis, PAMV represents the "mean level" of tumor angiogenesis in the non-necrotic area, while DCE-US quantitative parameters measure tumor perfusion as a whole. To improve the comparability of pathological and contrast parameters, we introduced the "tumor activity area ratio" to the weight PAMV to assess the "average" neovascularization levels of tumor segments containing necrotic areas (Fig. 4). To our knowledge, this method has not yet been reported in the literature.

In addition, as one of the key initiators of tumor angiogenesis, VEGF is overexpressed in a vast majority of solid tumors [31]. VEGF inhibitors are also important in anti-angiogenic therapy development. Bevacizumab, the first anti-angiogenic inhibitor, is effective in metastatic colorectal cancer, cervical cancer, ovarian cancer as well as lung cancer with chemotherapy [32]. Hence, the assessment of VEGF expression could be used to not only help disease diagnosis but also assess the anti-angiogenesis response. Moreover, the evaluation of VEGF is not limited to "hot spots", which makes it another parameter in tumor angiogenesis in the present study. For the same reason mentioned above, we also weighted VEGF scores by the "tumor activity area ratio". The results showed that weighted VEGF was positively correlated with the weighted PAMV score ($r = 0.90$, $P < 0.05$), indicating that weighted pathological parameters could effectively reflect tumor neovascularization.

To date, several studies have shown that quantitative 2D DCE-US PI was positively correlated with MVD and could be used to assess neovascularization in tumors, such as thyroid cancer and invasive breast cancer [30, 33], while Lucidarme O. et al. found no correlation between MVD or PAMV and contrast agent-based TIC parameters of 2D DCE-US in a murine model [34]. In the present study, the parameters of quantitative 2D DCE-US were not significantly correlated with weighted PAMV or VEGF, suggesting, on the one hand, that weighted PAMV and VEGF other than MVD should be used to evaluate tumor angiogenesis, and these new indices showed better correlations with DCE-US quantitative parameters. On the other hand, quantitative

parameters of 2D DCE-US were not as reproducible as those of 3D; hence their correlation with pathological parameters could be influenced by plane-to-plane sample error.

We acknowledge several limitations of the present study. First, the number of rabbits was small. Although the difference between quantitative 2D and 3D DCE-US was obvious, the results based on a larger sample size could be more credible. Second, we only discussed the feasibility, stability and accuracy of quantitative analysis without using 3D DCE-US in treatment response assessment in orthotopic animal models, which would verify the results of former studies using subcutaneous cancer xenografts models [13, 14]. Third, we used bolus DCE-US, based on the wash-in/wash-out kinetics of microbubbles after bolus injection, to compare 2D with 3D DCE-US. According to Wang et al. and El Kaffas, although both bolus and destruction–replenishment DCE-US showed good stability, the latter technique had a higher accuracy, this method was not influenced by indicator input function at the tumor [13, 15]. Further studies comparing both methods in orthotopically implanted tumor models are needed. What is more, all slides assessed pathologically when 3D-US images compared to pathological findings is the most optimized. But from the perspective of experimental funding and experimental technical feasibility, we only use a single level.

In conclusion, the present study indicates that the feasibility, stability and accuracy of 3D DCE-US were better than that of 2D for quantitative analysis. 3D DCE-US technique is a non-invasive method to evaluate tumor angiogenesis for cancer diagnosis.

Funding Funding was provided by Natural Science Foundation of China (Grant no. 81601500), Natural Science Foundation of Guangdong Province (Grant nos. 2017A030313661, 2016A030310143), Medical Science and Technology Foundation of Guangdong Province (Grant no. 2017A020215195)

Compliance with ethical standards

Ethical approval All animal experiments were complied with the ARRIVE guidelines and carried out in accordance with the National Institutes of Health guide for the care and use of Laboratory animals. All applicable institutional and national guidelines for the care and use of animals were followed.

Conflict of interest The authors declare that they have no conflict of interest.

References

1. Folkman J. What is the evidence that tumors are angiogenesis dependent? J Natl Cancer Inst. 1990;82(1):4–6.
2. Duffaud F, Therasse P. New guidelines to evaluate the response to treatment in solid tumors. Bull Cancer. 2000;87(12):881–6.
3. Marcus C, Ladam-Marcus V, Cucu C, Bouché O, Lucas L, Hoeffel C. Imaging techniques to evaluate the response to treatment in oncology: current standards and perspectives. Crit Rev Oncol Hematol. 2009;72(3):217–38.
4. Greis C. Ultrasound contrast agents as markers of vascularity and microcirculation. Clin Hemorheol Microcirc. 2009;43(1–2):1–9.
5. Greis C. Quantitative evaluation of microvascular blood flow by contrast-enhanced ultrasound (CEUS). Clin Hemorheol Microcirc. 2011;49(1–4):137–49.
6. Bartolotta TV, Midiri M, Galia M, et al. Qualitative and quantitative evaluation of solitary thyroid nodules with contrast-enhanced ultrasound: initial results. Eur Radiol. 2006;16(10):2234–41.
7. Ripolles T, Martinez MJ, Paredes JM, Blanc E, Flors L, Delgado F. Crohn disease: correlation of findings at contrast-enhanced US with severity at endoscopy. Radiology. 2009;253(1):241–8.
8. Wang JW, Cao LH, Han F, et al. Contrast-enhanced US quantitatively detects changes of tumor perfusion in a murine breast cancer model during adriamycin chemotherapy. Acta Radiol. 2013;54(8):882–8.
9. Zhang HP, Shi QS, Li F, et al. Regions of interest and parameters for the quantitative analysis of contrast-enhanced ultrasound to evaluate the anti-angiogenic effects of bevacizumab. Mol Med Rep. 2013;8(1):154–60.
10. Zhou JH, Cao LH, Zheng W, Liu M, Han F, Li AH. Contrast-enhanced gray-scale ultrasound for quantitative evaluation of tumor response to chemotherapy: preliminary results with a mouse hepatoma model. Am J Roentgenol. 2011;196(1):W13–W1717.
11. Williams R, Hudson J, Lloyd B, et al. Dynamic microbubble contrast-enhanced US to measure tumor response to targeted therapy: a proposed clinical protocol with results from renal cell carcinoma patients receiving antiangiogenic therapy. Radiology. 2011;260(2):581–90.
12. Lassau N, Bonastre J, Kind M, et al. Validation of dynamic contrast-enhanced ultrasound in predicting outcomes of antiangiogenic therapy for solid tumors the french multicenter support for innovative and expensive techniques study. Investig Radiol. 2014;49(12):794–800.
13. Wang HJ, Lutz AM, Hristov D, Tian L, Willmann JK. Intra-animal comparison between three-dimensional molecularly targeted US and three-dimensional dynamic contrast-enhanced US for early antiangiogenic treatment assessment in colon cancer. Radiology. 2017;282(2):443–52.
14. Zhou J, Zhang H, Wang H, et al. Early prediction of tumor response to bevacizumab treatment in murine colon cancer models using three-dimensional dynamic contrast-enhanced ultrasound imaging. Angiogenesis. 2017;20(4):547–55.
15. El Kaffas A, Sigrist RMS, Fisher G, et al. Quantitative three-dimensional dynamic contrast-enhanced ultrasound imaging: first-in-human pilot study in patients with liver metastases. Theranostics. 2017;7(15):3745–58.
16. Wang HJ, Hristov D, Qin JL, Tian L, Willmann JK. Three-dimensional dynamic contrast-enhanced US imaging for early antiangiogenic treatment assessment in a mouse colon cancer model. Radiology. 2015;277(2):424–34.
17. Yi CA, Lee KS, Kim EA, et al. Solitary pulmonary nodules: dynamic enhanced multi-detector row CT study and comparison with vascular endothelial growth factor and microvessel density. Radiology. 2004;233(1):191–9.
18. Lassau N, Koscielny S, Albiges L, et al. Metastatic renal cell carcinoma treated with sunitinib: early evaluation of treatment response using dynamic contrast-enhanced ultrasonography. Clin Cancer Res. 2010;16(4):1216–25.
19. Lassau N, Koscielny S, Chami L, et al. Advanced hepatocellular carcinoma: early evaluation of response to bevacizumab therapy at dynamic contrast-enhanced US with quantification-preliminary results. Radiology. 2011;258(1):291–300.

20. Feingold S, Gessner R, Guracar IM, Dayton PA. Quantitative volumetric perfusion mapping of the microvasculature using contrast ultrasound. Investig Radiol. 2010;45(10):669–74.
21. Williams R, Hudson JM, Lloyd BA, et al. Dynamic microbubble contrast-enhanced us to measure tumor response to targeted therapy: a proposed clinical protocol with results from renal cell carcinoma patients receiving antiangiogenic therapy. Radiology. 2011;260(2):581–90.
22. Wang Z, Wang W, Liu GJ, et al. The role of quantitation of real-time 3-dimensional contrast-enhanced ultrasound in detecting microvascular invasion: an in vivo study. Abdom Radiol (N Y). 2016;41(10):1973–9.
23. Ferraioli G, Meloni MF. Contrast-enhanced ultrasonography of the liver using SonoVue. Ultrasonography. 2018;37(1):25–35.
24. Weidner N, Semple JP, Welch WR, Folkman J. Tumor angiogenesis and metastasis-correlation in invasive breast carcinoma. N Engl J Med. 1991;324(1):1–8.
25. Uzzan B, Nicolas P, Cucherat M, Perret GY. Microvessel density as a prognostic factor in women with breast cancer: a systematic review of the literature and meta-analysis. Cancer Res. 2004;64(9):2941–55.
26. Weidner N. Tumor angiogenesis: review of current applications in tumor prognostication. Semin Diagn Pathol. 1993;10(4):302–13.
27. Macchiarini P, Fontanini G, Hardin MJ, Squartini F, Angeletti CA. Relation of neovascularisation to metastasis of non-small-cell lung cancer. Lancet (Lond Engl). 1992;340(8812):145–6.
28. Sharma S, Aggarwal N, Gupta S, Singh M, Gupta R, Dinda A. Angiogenesis in renal cell carcinoma: correlation of microvessel density and microvessel area with other prognostic factors. Int Urol Nephrol. 2011;43(1):125–9.
29. Shiyan L, Pintong H, Zongmin W, et al. The relationship between enhanced intensity and microvessel density of gastric carcinoma using double contrast-enhanced ultrasonography. Ultrasound Med Biol. 2009;35(7):1086–91.
30. Mori N, Mugikura S, Takahashi S, et al. Quantitative analysis of contrast-enhanced ultrasound imaging in invasive breast cancer: a novel technique to obtain histopathologic information of microvessel density. Ultrasound Med Biol. 2017;43(3):607–14.
31. Dvorak HF. Vascular permeability factor/vascular endothelial growth factor: a critical cytokine in tumor angiogenesis and a potential target for diagnosis and therapy. J Clin Oncol. 2002;20(21):4368–80.
32. Jayson GC, Kerbel R, Ellis LM, Harris AL. Antiangiogenic therapy in oncology: current status and future directions. Lancet. 2016;388(10043):518–29.
33. Wei X, Li Y, Zhang S, Ming G. Evaluation of thyroid cancer in Chinese females with breast cancer by vascular endothelial growth factor (VEGF), microvessel density, and contrast-enhanced ultrasound (CEUS). Tumour Biol. 2014;35(7):6521–9.
34. Lucidarme O, Kono Y, Corbeil J, et al. Angiogenesis: noninvasive quantitative assessment with contrast-enhanced functional US in murine model. Radiology. 2006;239(3):730–9.

Affiliations

Qiao Zheng[1] · Jian-chao Zhang[1] · Zhu Wang[1] · Si-Min Ruan[1] · Wei Li[1] · Fu-Shun Pan[1] · Li-Da Chen[1] · Yu-Chen Zhang[2] · Wen-Xin Wu[2] · Xiao-Yan Xie[1] · Ming-De Lu[1,3] · Quan-Yuan Shan[1] · Wei Wang[1]

Qiao Zheng
zhengq23@mail2.sysu.edu.cn

Jian-chao Zhang
zhangjch35@mail2.sysu.edu.cn

Zhu Wang
wangzhu@mail.sysu.edu.cn

Si-Min Ruan
ruansm@mail2.sysu.edu.cn

Wei Li
liwei259@mail.sysu.edu.cn

Fu-Shun Pan
panfushun123@163.com

Li-Da Chen
chenlda@mail.sysu.edu.cn

Yu-Chen Zhang
zhangych27@mail2.sysu.edu.cn

Wen-Xin Wu
wuwx6@mail2.sysu.edu.cn

Xiao-Yan Xie
xxy1992sys@163.com

Ming-De Lu
lumd@live.com

[1] Department of Medical Ultrasonics, Institute of Diagnostic and Interventional Ultrasound, The First Affiliated Hospital of Sun Yat-Sen University, No. 58 Zhongshan Road 2, Guangzhou 510080, People's Republic of China

[2] Zhongshan School of Medicine, Sun Yat-Sen University, No. 74 Zhongshan Road 2, Guangzhou 510080, People's Republic of China

[3] Department of Hepatobiliary Surgery, The First Affiliated Hospital of Sun Yat-Sen University, No. 58 Zhongshan Road 2, Guangzhou 510080, People's Republic of China